Query-Centric Trajectory Prediction

Zikang Zhou[1,2]   Jianping Wang[1,2]   Yung-Hui Li[3]   Yu-Kai Huang[4]

[1]City University of Hong Kong   [2]City University of Hong Kong Shenzhen Research Institute
[3]Hon Hai Research Institute   [4]Carnegie Mellon University

zikanzhou2-c@my.cityu.edu.hk

Abstract

Predicting the future trajectories of surrounding agents is essential for autonomous vehicles to operate safely. This paper presents QCNet, a modeling framework toward pushing the boundaries of trajectory prediction. First, we identify that the agent-centric modeling scheme used by existing approaches requires re-normalizing and re-encoding the input whenever the observation window slides forward, leading to redundant computations during online prediction. To overcome this limitation and achieve faster inference, we introduce a query-centric paradigm for scene encoding, which enables the reuse of past computations by learning representations independent of the global spacetime coordinate system. Sharing the invariant scene features among all target agents further allows the parallelism of multi-agent trajectory decoding. Second, even given rich encodings of the scene, existing decoding strategies struggle to capture the multimodality inherent in agents' future behavior, especially when the prediction horizon is long. To tackle this challenge, we first employ anchor-free queries to generate trajectory proposals in a recurrent fashion, which allows the model to utilize different scene contexts when decoding waypoints at different horizons. A refinement module then takes the trajectory proposals as anchors and leverages anchor-based queries to refine the trajectories further. By supplying adaptive and high-quality anchors to the refinement module, our query-based decoder can better deal with the multimodality in the output of trajectory prediction. Our approach ranks 1st on Argoverse 1 and Argoverse 2 motion forecasting benchmarks, outperforming all methods on all main metrics by a large margin. Meanwhile, our model can achieve streaming scene encoding and parallel multi-agent decoding thanks to the query-centric design ethos.

1. Introduction

Making safe decisions for autonomous vehicles requires accurate predictions of surrounding agents' future trajectories. In recent years, learning-based methods have been
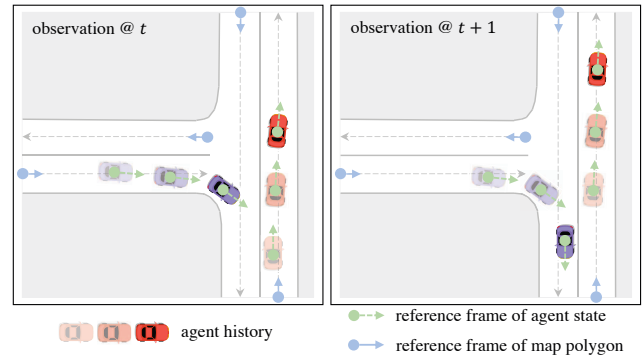

Figure 1. Illustration of our **query-centric reference frame**, where we build a local coordinate system for *each* spatial-temporal element, including map polygons and agent states at all time steps. In the attention-based encoder, all scene elements' queries are derived and updated in their local reference frames.

widely used for trajectory prediction [14, 31, 37, 38, 46, 56]. Despite the considerable efforts made to enhance models' forecasting ability, there is still a long way to go before fully addressing the problem of trajectory prediction. Why is this task so challenging, and what inability lies in existing approaches? We attempt to answer these questions from the following two perspectives:

(i) While the flourishing forecasting models have achieved impressive performance on trajectory prediction benchmarks [7, 13, 49], today's most advanced architectures specialized for this task [37, 38, 46, 56] fail to process the heterogeneous traffic scenes *efficiently*. In an autonomous driving system, data frames arrive at the prediction module sequentially as a stream of sparse scene context, including the high-definition vector map and the surrounding agents' kinematic states. A model must learn expressive representations of these scene elements to achieve accurate forecasts. With the continuing development of modeling techniques for sparse context encoding [14, 31, 50], the research community has witnessed rapid progress toward more powerful trajectory predictors. Notably, factorized attention-based Transformers [37, 38, 56] have recently raised prediction accuracy to an unprecedented level. However, they require learning attention-based representations for each spatial-

temporal scene element and suffer from prohibitively high costs when processing dense traffic scenes. As every minimal delay may lead to catastrophic accidents in autonomous driving, the unmet need for real-time predictions has limited the applicability of state-of-the-art approaches.

(ii) The immense uncertainty in the output of trajectory prediction, which grows explosively as the prediction horizon lengthens, has troubled the research community constantly. For example, a vehicle at an intersection may turn or go straight depending on the driver's long-term goal. To avoid missing any potential behavior, a model must learn to capture the underlying multimodal distribution rather than simply predicting the most frequent mode. This learning task is challenging since only one possibility is logged in each training sample. To ease the learning difficulty, a body of works utilizes handcrafted anchors as guidance for multimodal prediction [6, 12, 39, 53, 55]. Their effectiveness, however, is subject to the quality of the anchors. Typically, these methods fail to work well when few anchors can precisely cover the ground truth. This problem is exacerbated in long-term prediction, where the search space for anchors is much larger. Some other works [10, 31, 38, 46, 56] circumvent this issue by directly predicting multiple trajectories, albeit at the risk of mode collapse and training instability [33, 41]. Due to the lack of spatial priors, these methods also fail to produce accurate long-term forecasts.

The analysis above drives us to propose a trajectory prediction framework, termed as QCNet, to overcome the limitations of previous solutions. **First**, we note that it is possible to achieve faster online inference while also benefiting from the power of factorized attention, but the agent-centric encoding scheme [25, 27, 46, 56] used by existing methods serves as an impediment. Each time a new data frame arrives, the observation window slides one step forward and overlaps with its predecessor substantially, which provides opportunities for models to reuse the previously computed encodings. However, agent-centric approaches require normalizing the input based on the latest agent states' positions, necessitating the re-encoding of scene elements whenever the observation window slides forward. To address this issue, we introduce a *query-centric* paradigm for scene encoding (see Fig. 1). The crux of our design ethos lies in processing all scene elements in their local spacetime reference frames and learning representations independent of the global coordinates. This strategy enables us to cache and reuse the previously computed encodings, spreading the computation across all observation windows and thereby reducing inference latency. The invariant scene features can also be shared among all target agents in the scene to enable the parallelism of multi-agent decoding. **Second**, to better utilize the scene encodings for multimodal and long-term prediction, we use anchor-free queries to retrieve the scene context *recurrently* and let them decode a short seg-

ment of future waypoints at each recurrence. This recurrent mechanism eases the modeling burden on the queries by allowing them to focus on different scene contexts when predicting waypoints at different horizons. The high-quality trajectories predicted by the recurrent decoder serve as dynamic anchors in the subsequent refinement module, where we use anchor-based queries to refine the trajectory proposals based on the scene context. As a result, our query-based decoding pipeline incorporates the flexibility of anchor-free methods into anchor-based solutions, taking the best of both worlds to facilitate multimodal and long-term prediction.

Our proposed query-centric encoding paradigm is the first that can exploit the sequential nature of trajectory prediction to achieve fast online inference. Besides, our query-based decoder exhibits superior performance for multimodal and long-term prediction. Experiments show that our approach achieves state-of-the-art results, ranking 1st on two large-scale motion forecasting benchmarks [7, 49].

2. Related Work

Scene context fusion encodes rich information for trajectory prediction. Early work rasterizes world states as multichannel images and employs classic convolutional neural networks for learning [5, 6, 10, 21]. Due to the lossy rendering, limited receptive field, and prohibitively high cost of raster-based methods, the research community has turned to a vector-based encoding scheme [14, 31, 50]. With the use of permutation-invariant set operators such as pooling [3, 12, 14, 20, 46], graph convolution [11, 31, 36, 53], and attention mechanism [24, 26, 30, 32, 34, 52], vector-based methods can efficiently aggregate sparse information in traffic scenes. Several powerful trajectory prediction models have recently adopted Transformers [47] with factorized attention as their encoders [18, 37, 38, 56]. Although these models improve efficiency by learning agent-centric representations hierarchically [56] or encoding the whole scene in a shared coordinate system [38], their scalability is still limited by the computational complexity of factorized attention. In comparison, our encoder inherits the representational power of factorized attention while achieving more efficient scene context fusion by using a query-centric encoding paradigm, which goes beyond agent-centric modeling and enables streaming trajectory prediction.

Multimodal future distribution is a widely adopted output form of trajectory prediction, given that world states are partially observable and agents' intentions are highly uncertain. While generative models naturally fit multimodal prediction [20, 28, 40, 45], sampling from latent variables introduces test-time stochasticity, which is undesirable for safety-critical applications such as autonomous driving. Another line of research tackles multimodality by decoding a discrete set of trajectories from the encoded scene context [6, 10, 31, 55]. Since only one mode is ob-

served in training data, predicting multiple diverse futures is challenging. Anchor-based methods achieve this with the guidance of anchors, which facilitate multimodal prediction by leveraging predefined maneuvers [12], candidate trajectories [6, 39], or map-adaptive goals [53, 55]. However, the quality of these anchors significantly impacts prediction performance. By contrast, anchor-free methods output multiple hypotheses freely at the risk of mode collapse and training instability [10, 31, 38, 46]. Our decoding pipeline takes advantage of both anchor-based and anchor-free solutions, with an anchor-free module generating adaptive anchors in a data-driven manner and an anchor-based module refining these anchors based on the scene context.

3. Approach

3.1. Input and Output Formulation

Consider a scenario with A agents surrounding the autonomous vehicle. During online running, the perception module supplies a stream of agent states to the prediction module at a fixed interval, where each agent state is associated with its spatial-temporal position and geometric attributes. For example, the i-th agent's state at time step t comprises the spatial position $\mathbf{p}_i^t = (\mathbf{p}_{i,x}^t, \mathbf{p}_{i,y}^t)$, the angular position $\boldsymbol{\theta}_i^t$ (*i.e.*, the yaw angle), the temporal position t (*i.e.*, the time step), and the velocity $\mathbf{v}_i^t$. We also add the motion vector $\mathbf{p}_i^t - \mathbf{p}_i^{t-1}$ to the geometric attributes similar to some baselines [31, 56]. Besides, the prediction module has access to M polygons on the high-definition map (*e.g.*, lanes and crosswalks), where each map polygon is annotated with sampled points and semantic attributes (*e.g.*, the user type of a lane). Given the map information and the agent states within an observation window of T time steps, the prediction module is tasked with forecasting K future trajectories for each target agent over a horizon of T' time steps and assigning a probability score for each forecast.

3.2. Query-Centric Scene Context Encoding

The first step of trajectory prediction is to encode the scene input. Recent research has found factorized attention incredibly effective for scene encoding [37, 38, 56]. These approaches let a query element attend to key/value elements along one axis at a time, which results in temporal attention, agent-map attention, and social attention (*i.e.*, agent-agent attention) with the complexity of $\mathcal{O}(AT^2)$, $\mathcal{O}(ATM)$, and $\mathcal{O}(A^2T)$, respectively. Unlike typical encoding strategies that first apply a temporal network to squeeze the time dimension and then perform agent-map and agent-agent fusions at the current time step only, factorized attention conducts fusions at *every* past time step within the observation window. As a result, factorized attention can capture more information, such as how the relations between agents and map elements evolve over the observation horizon. How-

ever, its scalability is limited by the cubic complexity of each fusion operation. In extreme circumstances involving hundreds of agents and map elements, such models may fail to emit predictions promptly. We ask: *is it possible to reduce the inference latency during online prediction while enjoying the representational power of factorized attention?*

Before diving into our solution, recall that trajectory prediction is a streaming processing task: when a new data frame arrives, we put it in the queue and drop the oldest one. Thus, the latest observation window has $T-1$ time steps overlapping with its predecessor. This fact motivates us to raise another question: *can we reuse the overlapped time steps' encodings computed previously after the observation window slides forward?* Unfortunately, this idea is infeasible owing to the normalization requirement for trajectory prediction: existing methods employ an agent-centric encoding paradigm for spatially roto-translation invariance [25, 27, 46, 56], where each agent is encoded in the local coordinate frame determined by its *current* time step's position and yaw angle. Each time the observation window slides forward, the "current time step" also shifts accordingly, and the geometric attributes of all scene elements need to be re-normalized based on the positions of the latest agent states. Due to the variation in input, we are forced to re-encode all time steps' elements even though the observation windows largely overlap.

Based on the analysis above, we identify that the evolving spacetime coordinate systems hinder the reuse of previously computed encodings. To address this issue, we introduce a query-centric encoding paradigm for learning representations independent of scene elements' global coordinates. Specifically, we establish a local spacetime coordinate system for *each* scene element that a query vector derives from, processing query elements' features in their local reference frames. Then, we inject the relative spatial-temporal positions into the key and value elements when performing attention-based scene context fusion. We elaborate on the encoding process in the following paragraphs.

Local Spacetime Coordinate System. Figure 1 shows an example of scene elements' local coordinate systems. For the i-th agent's state at time step t, the local coordinate frame is determined by the reference spatial-temporal position $(\mathbf{p}_i^t, t)$ and the reference direction $\boldsymbol{\theta}_i^t$, where $\mathbf{p}_i^t$ and $\boldsymbol{\theta}_i^t$ are the agent state's spatial and angular positions, respectively. For lanes and crosswalks, we choose the position and orientation at the entry point of the centerline as the reference. In this way, we build local coordinate systems canonically for all the scene elements considered, resulting in one dedicated local frame per map polygon and T reference frames per agent within any observation window.

Scene Element Embedding. For each spatial-temporal scene element, such as an agent state or a lane, we compute the polar coordinates of all geometric attributes (*e.g.*,

17865

the velocity and motion vector of an agent state, the positions of all sampled points on a lane) relative to the spatial point and direction referenced by the element's local frame. Then, we transform each polar coordinate into Fourier features [22, 35, 44] to facilitate learning high-frequency signals. For each agent state and each sampled point on the map, the Fourier features are concatenated with the semantic attributes (*e.g.*, an agent's category) and passed through a multi-layer perceptron (MLP) to obtain an embedding. To further produce polygon-level representations for lanes and crosswalks, we apply attention-based pooling on the embeddings of sampled points within each map polygon. These operations result in agent embeddings of shape $[A, T, D]$ and map embeddings of shape $[M, D]$, where D denotes the hidden feature dimension. Benefiting from modeling in local reference frames, the embedding of each agent state/map polygon has only one instance and can be reused in the subsequent observation windows. In contrast, agent-centric approaches have to copy all inputs multiple times, encode each copy relative to one of the A agents' current position and heading, and re-encode all inputs whenever the observation window slides forward, leading to much more overhead during online inference.

Relative Spatial-Temporal Positional Embedding. We prepare the relative positional embeddings for scene element pairs, which will be incorporated into the attention-based operators to help the model be aware of the difference between two elements' local coordinate frames. For an element with absolute spatial-temporal position $(\mathbf{p}_i^t, \boldsymbol{\theta}_i^t, t)$ and another with $(\mathbf{p}_j^s, \boldsymbol{\theta}_j^s, s)$, we use a 4D descriptor to summarize their relative position, whose components are the relative distance $\left\|\mathbf{p}_j^s - \mathbf{p}_i^t\right\|_2$, the relative direction $\mathrm{atan2}(\mathbf{p}_{j,y}^s - \mathbf{p}_{i,y}^t, \ \mathbf{p}_{j,x}^s - \mathbf{p}_{i,x}^t) - \boldsymbol{\theta}_i^t$, the relative orientation $\boldsymbol{\theta}_j^s - \boldsymbol{\theta}_i^t$, and the time gap $s - t$. Since we can easily reconstruct one element's absolute position from another with the help of the descriptor, we have preserved all spatial-temporal position information of the scene element pair. Then, we transform the 4D descriptor into Fourier features and pass them through an MLP to produce the relative positional embedding $\mathbf{r}_{j \to i}^{s \to t}$. If any of the two scene elements are static (*e.g.*, static map polygons), we can omit the superscript and denote the embedding as $\mathbf{r}_{j \to i}$.

Self-Attention for Map Encoding. We employ self-attention to model the relationships among map elements, after which the updated map encodings will enrich the agent features and assist trajectory decoding. For the i-th map polygon, we derive a query vector from its embedding $\mathbf{m}_i$ and let it attend to the neighboring lanes and crosswalks $\{\mathbf{m}_j\}_{j \in \mathcal{N}_i}$, where $\mathcal{N}_i$ denotes the neighbor set of the polygon. To incorporate spatial awareness for map encoding, we generate the j-th key/value vector from the concatenation of $\mathbf{m}_j$ and the relative positional embedding, *i.e.*, $[\mathbf{m}_j; \mathbf{r}_{j \to i}]$. Since each triple of $(\mathbf{m}_i, \mathbf{m}_j, \mathbf{r}_{j \to i})$ input to the attention
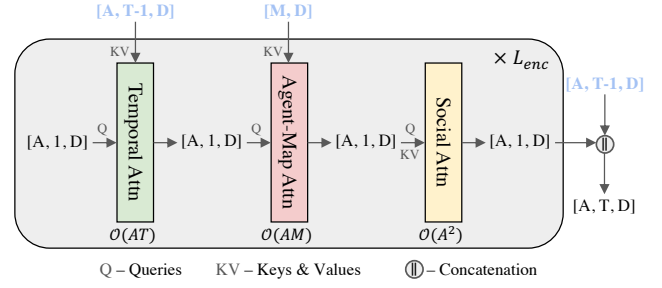

Figure 2. Overview of the **encoder** in an online mode. After reusing the encodings computed in previous observation windows (blue), the complexity of factorized attention goes from $\mathcal{O}(AT^2) + \mathcal{O}(ATM) + \mathcal{O}(A^2T)$ to $\mathcal{O}(AT) + \mathcal{O}(AM) + \mathcal{O}(A^2)$.

layer is independent of the global spacetime coordinate system, the output map encodings $\{\mathbf{m}_i'\}_{i=1}^M$ are also invariant under transformations of the global reference frame. Thus, they can be shared across *all agents and all time steps* and can even be pre-computed offline, thereby avoiding redundant computation suffered by agent-centric modeling.

Factorized Attention for Agent Encoding. To help the agent embeddings capture more information, we also consider factorized attention across agent time steps, among agents, and between agents and maps. Take the i-th agent at time step t as an example. Given the query vector derived from the agent state's embedding $\mathbf{a}_i^t$, we employ temporal attention by computing the key and value vectors based on $\{[\mathbf{a}_i^s; \mathbf{r}_{i \to i}^{s \to t}]\}_{s=t-\tau}^{t-1}$, which are the i-th agent's embeddings from time step $t-\tau$ $(0 < \tau < T)$ to time step $t-1$ and the corresponding relative positional embeddings. Likewise, the key and value vectors for agent-map and social attention are derived from $\{[\mathbf{m}_j'; \mathbf{r}_{j \to i}]\}_{j \in \mathcal{N}_i}$ and $\{[\mathbf{a}_j^t; \mathbf{r}_{j \to i}^{t \to t}]\}_{j \in \mathcal{N}_i}$, respectively, where the neighbor set $\mathcal{N}_i$ is determined by a distance threshold of 50 meters. As a result of updating the initially invariant queries with invariant keys and values, the outputs of these layers are also invariant. We stack the temporal, the agent-map, and the social attention sequentially as one fusion block and repeat such blocks L_{enc} times.

Thanks to the query-centric modeling, all the agent and map encodings are unique and fixed no matter from which spacetime coordinate system we view them (*i.e.*, roto-translation invariance for the space dimension and translation invariance for the time dimension), enabling the model to reuse past computations and operate streamingly. During online prediction, we can cache the encodings computed in previous observation windows and incrementally update the scene representation. As shown in Fig. 2, our model only performs factorized attention for the A incoming agent states when a new data frame arrives, resulting in temporal attention with $\mathcal{O}(AT)$ complexity, agent-map attention with $\mathcal{O}(AM)$ complexity, and social attention with $\mathcal{O}(A^2)$ complexity. All of these operations are an order less expensive than their non-streaming counterpart. Finally, we update the cached tensors using the newly computed encodings.
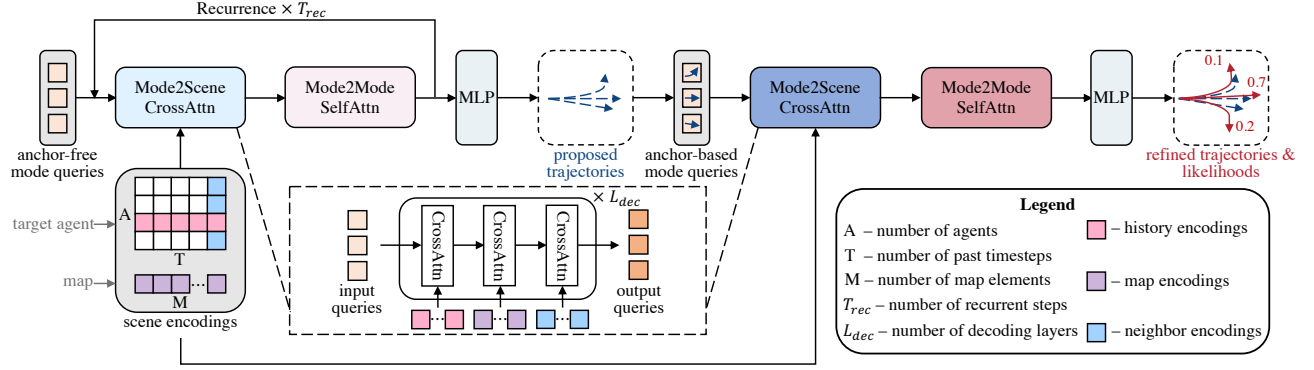
Figure 3. Overview of the **decoding pipeline**. An anchor-free module generates trajectory proposals *recurrently* based on the encoded scene context. These proposals act as the anchors in the refinement module, where an anchor-based decoder refines the anchor trajectories and assigns a probability score for each hypothesis.

3.3. Query-Based Trajectory Decoding

The second step of trajectory prediction is to utilize the scene encodings output by the encoder to decode K future trajectories for each target agent, which is non-trivial since the encoder returns only one set of feature embeddings. Inspired by the progress in object detection, some recent works [18, 32, 37, 46] employ DETR-like decoders [4] to deal with such a one-to-many problem, where multiple learnable queries cross-attend the scene encodings and decode trajectories. However, these models suffer from training instability and mode collapse like other anchor-free approaches. Moreover, they do not perform well in long-term prediction, where the forecasting task is much more challenging due to the explosive uncertainty in the distant future. Our query-based decoder overcomes these limitations by utilizing a recurrent, anchor-free proposal module to generate adaptive trajectory anchors, followed by an anchor-based module that further refines the initial proposals. An overview of our decoding pipeline is shown in Fig. 3. In the following, we will illustrate the components of the decoder in detail.

Mode2Scene and Mode2Mode Attention. Both the proposal and refinement modules use a DETR-like architecture. Similar to the concept of object queries in DETR [4], each query takes charge of decoding one of the K trajectory modes. In the Mode2Scene attention, we use cross-attention layers to update the mode queries with multiple contexts, including the history encodings of the target agent, the map encodings, and the neighboring agents' encodings. Following the Mode2Scene attention, the K mode queries "talk" to each other via the Mode2Mode self-attention to improve the diversity of multiple modes.

Reference Frames of Mode Queries. To predict the trajectories of multiple agents in parallel, we share the same set of scene encodings among all target agents in the scene. As these encodings are derived from their local spacetime coordinate systems, we need to project them into each target agent's current viewpoint to achieve the same effect as

agent-centric modeling. To this end, we hallucinate a coordinate frame for each mode query based on the corresponding target agent's current position and yaw angle. When updating the query embeddings via Mode2Scene attention, the scene elements' positions relative to the queries are incorporated into the keys and values, which is similar to what we have done for the encoder.

Anchor-Free Trajectory Proposal. We use learnable, anchor-free queries to propose initial trajectories. These proposals will later act as anchors in the refinement module. Compared with anchor-based methods that attempt to cover the ground truth with densely sampled handcrafted anchors [6, 19], our proposal module generates K adaptive anchors in a data-driven manner. Thanks to the cross-attention layers, the mode queries can retrieve the scene context and quickly narrow the search space for anchors. The self-attention layer further allows the queries to collaborate with each other when generating trajectory proposals.

Over an extended prediction horizon, an agent can travel a long distance, and its surrounding environment may vary quickly. As a result, it is hard to summarize all information required for decoding a long sequence into a single query embedding. To ease the queries' burden of context extraction and improve the anchors' quality, we generalize the DETR-like decoder to a *recurrent* fashion. Using T_{rec} recurrent steps, the context-aware mode queries only decode T'/T_{rec} future waypoints via an MLP at the end of each recurrent step. At the subsequent recurrence, these queries become the input again and extract the scene context relevant to the next few waypionts' prediction. For efficiency, T_{rec} is far smaller than the prediction horizon T'. We also find that using much more recurrent steps is unnecessary.

Anchor-Based Trajectory Refinement. Anchor-free decoding can be a two-edged sword: despite its flexibility, the unstable training process may lead to mode collapse occasionally. On the other hand, the randomly initialized mode queries must adapt to all target agents in all scenes and lack the scenario-specific bias, which may result in non-

compliant predictions, such as trajectories that violate the laws of motion or break the traffic rules conveyed by the high-definition map. We are thus motivated to employ an anchor-based module to refine the proposals further. Taking the output of the proposal module as anchors, we let the refinement module predict the offset to the proposed trajectories and estimate the likelihood of each hypothesis. This module also adopts a DETR-like architecture, but its mode queries are derived from the proposed trajectory anchors instead of randomly initialized. Specifically, a small GRU [8] is used to embed each trajectory anchor, and we take its final hidden state as the mode query. These anchor-based queries provide explicit spatial prior for the model, enabling the attention layers to localize the context of interest more easily.

3.4. Training Objectives

Following HiVT [56], we parameterize the i-th agent's future trajectory as a mixture of Laplace distributions:

$$f(\{\mathbf{p}_i^t\}_{t=1}^{T'}) = \sum_{k=1}^{K} \pi_{i,k} \prod_{t=1}^{T'} \text{Laplace}\left(\mathbf{p}_i^t \mid \boldsymbol{\mu}_{i,k}^t, \mathbf{b}_{i,k}^t\right), \quad (1)$$

where $\{\pi_{i,k}\}_{k=1}^{K}$ are the mixing coefficients, and the k-th mixture component's Laplace density at time step t is parameterized by the location $\boldsymbol{\mu}_{i,k}^t$ and the scale $\mathbf{b}_{i,k}^t$. We then use a classification loss $\mathcal{L}_{\text{cls}}$ to optimize the mixing coefficients predicted by the refinement module. This loss minimizes the negative log-likelihood of Eq. (1), and we stop the gradients of the locations and scales to optimize the mixing coefficients only. On the other hand, we adopt the winner-take-all strategy [29] to optimize the locations and scales output by the proposal and refinement modules, which conducts backpropagation on the best-predicted proposal and its refinement only. For stabilization, the refinement module stops the gradients of the proposed trajectory anchors. The final loss function combines the trajectory proposal loss $\mathcal{L}_{\text{propose}}$, the trajectory refinement loss $\mathcal{L}_{\text{refine}}$, and the classification loss $\mathcal{L}_{\text{cls}}$ for end-to-end training:

$$\mathcal{L} = \mathcal{L}_{\text{propose}} + \mathcal{L}_{\text{refine}} + \lambda \mathcal{L}_{\text{cls}}, \quad (2)$$

where we use λ to balance regression and classification.

4. Experiments

4.1. Experimental Settings

Datasets. We use Argoverse 1 [7] and Argoverse 2 [49], two large-scale motion forecasting datasets, to test the efficacy of our approach. The Argoverse 1 dataset collects $323,557$ sequences of data from Miami and Pittsburgh, while the Argoverse 2 dataset contains $250,000$ scenarios spanning six cities. Both datasets have a sampled rate of 10 Hz. For the Argoverse 1 dataset, models need to predict agents' 3-second future trajectories given the 2-second

observations of history. The Argoverse 2 dataset, in comparison, is featured by improved data diversity, higher data quality, a larger observation window of 5 seconds, and a longer prediction horizon of 6 seconds. Using these two datasets, we intend to examine models' forecasting capability on various data distributions and prediction horizons.

Metrics. Following the standard evaluation protocol, we adopt metrics including minimum Average Displacement Error (minADE$_K$), minimum Final Displacement Error (minFDE$_K$), Brier-minimum Final Displacement Error (b-minFDE$_K$), and Miss Rate (MR$_K$) for evaluation. The metric minADE$_K$ calculates the ℓ_2 distance in meters between the ground-truth trajectory and the best of K predicted trajectories as an average of all future time steps. On the other hand, the metric minFDE$_K$ only concerns the prediction error at the final time step to emphasize long-term performance. To further measure the performance of uncertainty estimation, the metric b-minFDE$_K$ adds $(1 - \hat{\pi})^2$ to the final-step error, where $\hat{\pi}$ denotes the best-predicted trajectory's probability score that the model assigns. Moreover, the metric MR$_K$ is used for counting the ratio of cases where minFDE$_K$ exceeds 2 meters. As a common practice, K is selected as 1 and 6. If a model outputs more than K trajectories, only the predictions with the top-K probability scores are considered during evaluation.

4.2. Comparison with State of the Art

We compare our method with the strongest baselines on the Argoverse 1 and the Argoverse 2 motion forecasting benchmarks [7, 49]. We first conduct experiments on the Argoverse 2 dataset [49], which favors solutions that work well on long-term prediction, given that its prediction horizon is as long as 6 seconds. The results are shown in Tab. 1. Even without ensembling, QCNet has already outperformed all previous approaches on the Argoverse 2 test set in terms of minADE$_6$, minFDE$_6$, minADE$_1$, and minFDE$_1$. After using ensembling techniques similar to other entries, QCNet surpasses all methods on all metrics by a large margin. We also evaluate our model on the Argoverse 1 dataset [7] to better understand the generalizability of our approach. Although the performance on the Argoverse 1 benchmark has saturated for years [49], Tab. 2 shows that QCNet significantly advances state-of-the-art on most metrics. As of the time we submitted the paper, QCNet ranks 1st on the leaderboards of Argoverse 1 and Argoverse 2, outperforming all published and unpublished works on the two benchmarks. Please refer to the supplementary material for more results on Argoverse 2 [49] and Waymo Open Motion Dataset [13].

4.3. Ablation Study

Effects of Scene Context Fusion. We study the effects of scene context fusion in Tab. 3. The first question we answer is whether factorized attention is worth it. If no fac-

Method	b-minFDE$_6$ ↓	minADE$_6$ ↓	minFDE$_6$ ↓	MR$_6$ ↓	minADE$_1$ ↓	minFDE$_1$ ↓	MR$_1$ ↓
THOMAS [17]	2.16	0.88	1.51	0.20	1.95	4.71	0.64
GoRela [9]	2.01	0.76	1.48	0.22	1.82	4.62	0.66
MTR [42]	1.98	0.73	1.44	<u>0.15</u>	1.74	4.39	<u>0.58</u>
GANet [48]	1.96	0.72	1.34	0.17	1.77	4.48	0.59
QML* [43]	1.95	0.69	1.39	0.19	1.84	4.98	0.62
BANet* [54]	1.92	0.71	1.36	0.19	1.79	4.61	0.60
QCNet (w/o ensemble)	<u>1.91</u>	<u>0.65</u>	<u>1.29</u>	0.16	<u>1.69</u>	<u>4.30</u>	0.59
QCNet (w/ ensemble)	**1.78**	**0.62**	**1.19**	**0.14**	**1.56**	**3.96**	**0.55**

Table 1. Quantitative results on the **Argoverse 2** motion forecasting leaderboard [1] ranked by b-minFDE$_6$. Baselines that are known to have used ensembling are marked with symbol "*". For each metric, the best result is in **bold** and the second best result is underlined.

Method	b-minFDE$_6$↓	minADE$_6$↓	minFDE$_6$↓	MR$_6$↓
LaneGCN [31]	2.06	0.87	1.36	0.16
mmTransformer [32]	2.03	0.84	1.34	0.15
DenseTNT [19]	1.98	0.88	1.28	0.13
TPCN [50]	1.93	0.82	1.24	0.13
SceneTransformer [38]	1.89	0.80	1.23	0.13
HOME+GOHOME [15, 16]	1.86	0.89	1.29	**0.08**
HiVT [56]	1.84	0.77	1.17	0.13
MultiPath++ [46]	1.79	0.79	1.21	0.13
GANet [48]	1.79	0.81	1.16	0.12
PAGA [11]	1.76	0.80	1.21	0.11
DCMS [51]	1.76	0.77	1.14	0.11
Wayformer [37]	1.74	0.77	1.16	0.12
Ours	**1.69**	**0.73**	**1.07**	0.11

Table 2. Quantitative results on the **Argoverse 1** motion forecasting leaderboard [2]. The leaderboard is sorted by b-minFDE$_6$.

Model	Online Inference (ms) w/o reuse	w/ reuse	minADE$_6$↓	minFDE$_6$↓	MR$_6$↓
QCNet ($L_{enc} = 0$)	8±1	1±0	0.76	1.33	0.18
QCNet ($L_{enc} = 1$)	64±1	10±1	0.74	1.30	0.17
QCNet ($L_{enc} = 2$)	82±1	13±1	**0.73**	**1.27**	**0.16**

Table 3. Models' performance and inference latency evaluated on the Argoverse 2 validation set. We use an A40 GPU to measure encoders' online inference latency in the **densest** traffic scene involving **190** agents and **169** map polygons.

torized attention-based fusion blocks are employed, the encoder does not involve information interactions along different axes of the scene. Even so, the decoder has access to all information required for predictions thanks to the Mode2Scene layers. As shown in the first row of Tab. 3, our model can offer solid prediction performance without fusing the scene context. But after feeding our decoder with the fused encodings, the model gains considerable improvement over its non-fusion variant. Moreover, increasing the number of fusion blocks yields better results on all metrics, demonstrating the effectiveness of factorized attention. However, the resulting inference latency is not amenable to real-time applications such as autonomous driving, making this modeling choice less appealing for widespread adoption. Fortunately, our query-centric paradigm allows the reuse of computations from previous observation windows during online prediction, which goes beyond agent-centric approaches such as HiVT [56]. As shown in Tab. 3, caching

and reusing the previously computed encodings drastically lowers the online inference latency in the densest traffic scene. Such a "free lunch" also provides headroom to design a more advanced decoder for stronger performance.

Component Study of the Decoder. As demonstrated in Tab. 4, all layers in the decoder contribute to the performance to a certain degree. First, although the factorized attention in the encoder has already brought context awareness to the agent features, we find that using the target agent's history encodings alone is insufficient for accurate trajectory proposals. We hypothesize that injecting the map and social information into the anchor-free decoder can explicitly provide the queries with the future context, enabling them to narrow the search space for initial trajectories. On the other hand, the map and social information can also help the anchor-based queries identify those unrealistic predictions, such as trajectories that break the traffic rules or collide with static objects on the road. As a result, the role of our refinement module is more than simply trajectory smoothing [23, 51]. Table 4 also shows that removing the Mode2Mode self-attention in either the proposal or the refinement module will harm the long-term accuracy and the diversity of multiple hypotheses.

Table 5 demonstrates the effects of the recurrent mechanism and the refinement module on different datasets. On Argoverse 1, most agents merely exhibit trivial behavior, and the scene context usually does not have significant variation within the 3-second prediction horizon. For this reason, our design choices only bring marginal improvement when evaluated on this dataset. However, on the more challenging Argoverse 2 dataset where the prediction horizon is 6 seconds, increasing the number of recurrent steps from 1 (*i.e.*, no recurrence) to 3 leads to much better long-term performance, and the refinement module offers a dramatic improvement in terms of both accuracy and multimodality. We also notice that using much more recurrent steps is redundant: when increasing the number from 3 to 6, the model performance on Argoverse 2 cannot be further improved.

4.4. Qualitative Results

We present some qualitative results on the Argoverse 2 validation set. Comparing Fig. 4a and Fig. 4b, we can see

	Proposal Module				Refinement Module			b-minFDE$_6\downarrow$	minADE$_6\downarrow$	minFDE$_6\downarrow$	MR$_6\downarrow$
Time	Map	Social	Mode	Time	Map	Social	Mode				
✓			✓					2.22	0.82	1.58	0.22
✓	✓		✓					2.04	0.78	1.43	0.19
✓		✓	✓					2.18	0.81	1.55	0.22
✓	✓	✓						2.06	0.79	1.48	0.21
✓	✓	✓	✓					2.02	0.77	1.40	0.19
✓	✓	✓	✓	✓			✓	1.99	0.74	1.33	0.17
✓	✓	✓	✓	✓	✓		✓	1.94	0.74	1.30	0.17
✓	✓	✓	✓	✓		✓	✓	1.97	0.74	1.31	0.17
✓	✓	✓	✓	✓	✓	✓		1.91	**0.73**	1.29	0.17
✓	✓	✓	✓	✓	✓	✓	✓	**1.90**	**0.73**	**1.27**	**0.16**

Table 4. Ablation study on the components of the decoder. Experimental results are based on the Argoverse 2 validation set.
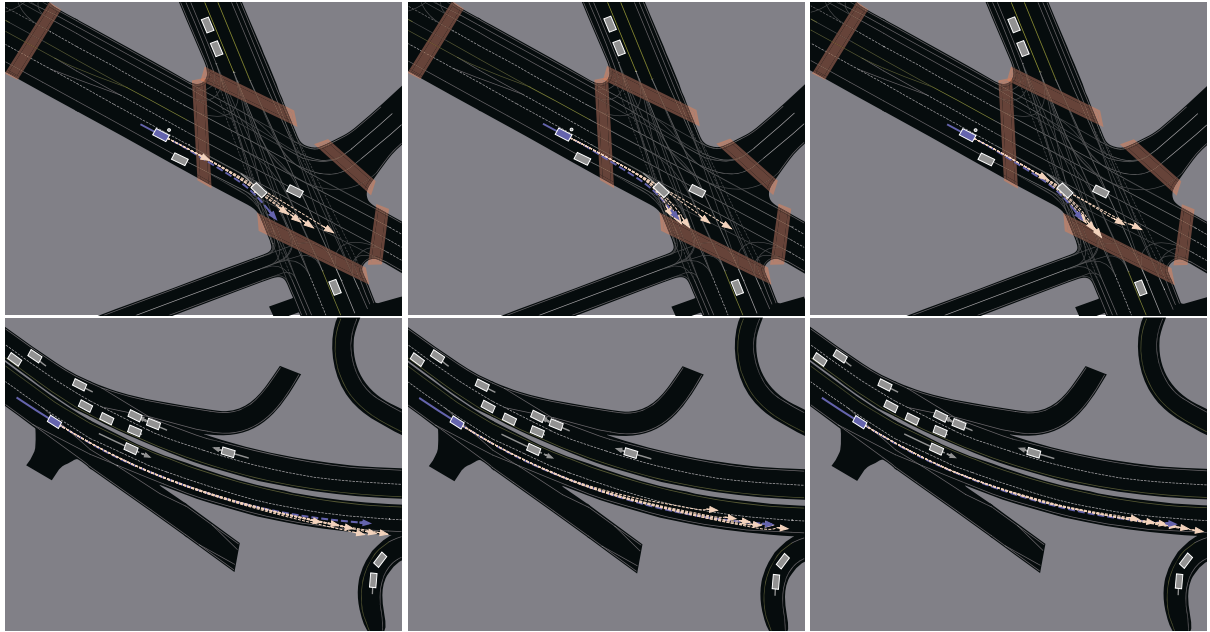
(a) w/o recurrence & w/o refinement   (b) w/ recurrence & w/o refinement   (c) w/ recurrence & w/ refinement

Figure 4. Qualitative results on the Argoverse 2 validation set. The target agents' bounding boxes and ground-truth trajectories are shown in purple, and models' predictions are shown in pink.

Dataset	#Recurrent Step	Refinement	b-minFDE$_6\downarrow$	minFDE$_6\downarrow$	MR$_6\downarrow$
Argoverse 1 (3-sec pred.)	1 (3 sec/step)	×	1.58	0.92	0.09
	2 (1.5 sec/step)	×	1.57	0.90	0.08
	3 (1 sec/step)	×	1.56	0.90	0.08
	3 (1 sec/step)	✓	**1.55**	**0.89**	0.08
Argoverse 2 (6-sec pred.)	1 (6 sec/step)	×	2.10	1.47	0.20
	2 (3 sec/step)	×	2.04	1.42	0.19
	3 (2 sec/step)	×	2.02	1.40	0.19
	3 (2 sec/step)	✓	**1.90**	**1.27**	**0.16**
	6 (1 sec/step)	✓	**1.90**	**1.27**	**0.16**

Table 5. Effects of the trajectory proposal and refinement modules on datasets with varying difficulty levels and prediction horizons.

that the recurrent mechanism of the proposal module can reduce the prediction error in the long term. Figure 4c further demonstrates the effectiveness of the refinement module, which improves the diversity of multiple hypotheses and the smoothness of the predicted trajectories.

5. Conclusion

This paper introduces QCNet, a neural architecture that overcomes some important challenges in trajectory prediction. Powered by the design ethos of query-centric modeling, QCNet maintains the representational capability of factorized attention while enjoying much faster inference. It achieves multimodal and long-term prediction by employing a recurrent, anchor-free trajectory proposal module and an anchor-based refinement module. QCNet exhibits unprecedented performance on large-scale trajectory prediction datasets, demonstrating the effectiveness of its designs.

Acknowledgement

References

[1] Argoverse 2: Motion forecasting competition. https://eval.ai/web/challenges/challenge-page/1719/overview. Accessed: 2022-11-11. 7

[2] Argoverse motion forecasting competition. https://eval.ai/web/challenges/challenge-page/454/overview. Accessed: 2022-11-11. 7

[3] Alexandre Alahi, Kratarth Goel, Vignesh Ramanathan, Alexandre Robicquet, Li Fei-Fei, and Silvio Savarese. Social lstm: Human trajectory prediction in crowded spaces. In *Proceedings of the IEEE Conference on Computer Vision and Pattern Recognition (CVPR)*, 2016. 2

[4] Nicolas Carion, Francisco Massa, Gabriel Synnaeve, Nicolas Usunier, Alexander Kirillov, and Sergey Zagoruyko. End-to-end object detection with transformers. In *Proceedings of the European Conference on Computer Vision (ECCV)*, 2020. 5

[5] Sergio Casas, Wenjie Luo, and Raquel Urtasun. Intentnet: Learning to predict intention from raw sensor data. In *Proceedings of the Conference on Robot Learning (CoRL)*, 2018. 2

[6] Yuning Chai, Benjamin Sapp, Mayank Bansal, and Dragomir Anguelov. Multipath: Multiple probabilistic anchor trajectory hypotheses for behavior prediction. In *Proceedings of the Conference on Robot Learning (CoRL)*, 2019. 2, 3, 5

[7] Ming-Fang Chang, John Lambert, Patsorn Sangkloy, Jagjeet Singh, Slawomir Bak, Andrew Hartnett, De Wang, Peter Carr, Simon Lucey, Deva Ramanan, et al. Argoverse: 3d tracking and forecasting with rich maps. In *Proceedings of the IEEE/CVF Conference on Computer Vision and Pattern Recognition (CVPR)*, 2019. 1, 2, 6

[8] Kyunghyun Cho, Bart van Merrienboer, Çaglar Gülçehre, Dzmitry Bahdanau, Fethi Bougares, Holger Schwenk, and Yoshua Bengio. Learning phrase representations using rnn encoder-decoder for statistical machine translation. In *Proceedings of the 2014 Conference on Empirical Methods in Natural Language Processing (EMNLP)*, 2014. 6

[9] Alexander Cui, Sergio Casas, Kelvin Wong, Simon Suo, and Raquel Urtasun. Gorela: Go relative for viewpoint-invariant motion forecasting. *arXiv preprint arXiv:2211.02545*, 2022. 7

[10] Henggang Cui, Vladan Radosavljevic, Fang-Chieh Chou, Tsung-Han Lin, Thi Nguyen, Tzu-Kuo Huang, Jeff Schneider, and Nemanja Djuric. Multimodal trajectory predictions for autonomous driving using deep convolutional networks. In *Proceedings of the IEEE International Conference on Robotics and Automation (ICRA)*, 2019. 2, 3

[11] Fang Da and Yu Zhang. Path-aware graph attention for hd maps in motion prediction. In *Proceedings of the IEEE International Conference on Robotics and Automation (ICRA)*, 2022. 2, 7

[12] Nachiket Deo and Mohan M Trivedi. Convolutional social pooling for vehicle trajectory prediction. In *Proceedings of the IEEE Conference on Computer Vision and Pattern Recognition Workshops (CVPRW)*, 2018. 2, 3

[13] Scott Ettinger, Shuyang Cheng, Benjamin Caine, Chenxi Liu, Hang Zhao, Sabeek Pradhan, Yuning Chai, Ben Sapp, Charles R Qi, Yin Zhou, et al. Large scale interactive motion forecasting for autonomous driving: The waymo open motion dataset. In *Proceedings of the IEEE/CVF International Conference on Computer Vision (ICCV)*, 2021. 1, 6

[14] Jiyang Gao, Chen Sun, Hang Zhao, Yi Shen, Dragomir Anguelov, Congcong Li, and Cordelia Schmid. Vectornet: Encoding hd maps and agent dynamics from vectorized representation. In *Proceedings of the IEEE/CVF Conference on Computer Vision and Pattern Recognition (CVPR)*, 2020. 1, 2

[15] Thomas Gilles, Stefano Sabatini, Dzmitry Tsishkou, Bogdan Stanciulescu, and Fabien Moutarde. Home: Heatmap output for future motion estimation. In *Proceedings of the IEEE International Conference on Intelligent Transportation Systems (ITSC)*, 2021. 7

[16] Thomas Gilles, Stefano Sabatini, Dzmitry Tsishkou, Bogdan Stanciulescu, and Fabien Moutarde. Gohome: Graph-oriented heatmap output for future motion estimation. In *Proceedings of the IEEE International Conference on Robotics and Automation (ICRA)*, 2022. 7

[17] Thomas Gilles, Stefano Sabatini, Dzmitry Tsishkou, Bogdan Stanciulescu, and Fabien Moutarde. Thomas: Trajectory heatmap output with learned multi-agent sampling. In *Proceedings of the International Conference on Learning Representations (ICLR)*, 2022. 7

[18] Roger Girgis, Florian Golemo, Felipe Codevilla, Martin Weiss, Jim Aldon D'Souza, Samira Ebrahimi Kahou, Felix Heide, and Christopher Pal. Latent variable sequential set transformers for joint multi-agent motion prediction. In *Proceedings of the International Conference on Learning Representations (ICLR)*, 2022. 2, 5

[19] Junru Gu, Chen Sun, and Hang Zhao. Densetnt: End-to-end trajectory prediction from dense goal sets. In *Proceedings of the IEEE/CVF International Conference on Computer Vision (ICCV)*, 2021. 5, 7

[20] Agrim Gupta, Justin Johnson, Li Fei-Fei, Silvio Savarese, and Alexandre Alahi. Social gan: Socially acceptable trajectories with generative adversarial networks. In *Proceedings of the IEEE Conference on Computer Vision and Pattern Recognition (CVPR)*, 2018. 2

[21] Joey Hong, Benjamin Sapp, and James Philbin. Rules of the road: Predicting driving behavior with a convolutional model of semantic interactions. In *Proceedings of the IEEE/CVF Conference on Computer Vision and Pattern Recognition (CVPR)*, 2019. 2

[22] Andrew Jaegle, Felix Gimeno, Andy Brock, Oriol Vinyals, Andrew Zisserman, and Joao Carreira. Perceiver: General perception with iterative attention. In *Proceedings of the International Conference on Machine Learning (ICML)*, 2021. 4

[23] Xiaosong Jia, Li Chen, Penghao Wu, Jia Zeng, Junchi Yan, Hongyang Li, and Yu Qiao. Towards capturing the temporal dynamics for trajectory prediction: a coarse-to-fine approach. In *Proceedings of the Conference on Robot Learning (CoRL)*, 2022. 7

[24] Xiaosong Jia, Liting Sun, Masayoshi Tomizuka, and Wei Zhan. Ide-net: Interactive driving event and pattern extraction from human data. *IEEE Robotics and Automation Letters (RA-L)*, 2021. 2

[25] Xiaosong Jia, Liting Sun, Hang Zhao, Masayoshi Tomizuka, and Wei Zhan. Multi-agent trajectory prediction by combining egocentric and allocentric views. In *Proceedings of the Conference on Robot Learning (CoRL)*, 2021. 2, 3

[26] Xiaosong Jia, Penghao Wu, Li Chen, Hongyang Li, Yu Liu, and Junchi Yan. Hdgt: Heterogeneous driving graph transformer for multi-agent trajectory prediction via scene encoding. *arXiv preprint arXiv:2205.09753*, 2022. 2

[27] Miltiadis Kofinas, Naveen Nagaraja, and Efstratios Gavves. Roto-translated local coordinate frames for interacting dynamical systems. In *Advances in Neural Information Processing Systems (NeurIPS)*, 2021. 2, 3

[28] Namhoon Lee, Wongun Choi, Paul Vernaza, Christopher B Choy, Philip HS Torr, and Manmohan Chandraker. Desire: Distant future prediction in dynamic scenes with interacting agents. In *Proceedings of the IEEE Conference on Computer Vision and Pattern Recognition (CVPR)*, 2017. 2

[29] Stefan Lee, Senthil Purushwalkam Shiva Prakash, Michael Cogswell, Viresh Ranjan, David Crandall, and Dhruv Batra. Stochastic multiple choice learning for training diverse deep ensembles. In *Advances in Neural Information Processing Systems (NIPS)*, 2016. 6

[30] Lingyun Luke Li, Bin Yang, Ming Liang, Wenyuan Zeng, Mengye Ren, Sean Segal, and Raquel Urtasun. End-to-end contextual perception and prediction with interaction transformer. In *Proceedings of the IEEE/RSJ International Conference on Intelligent Robots and Systems (IROS)*, 2020. 2

[31] Ming Liang, Bin Yang, Rui Hu, Yun Chen, Renjie Liao, Song Feng, and Raquel Urtasun. Learning lane graph representations for motion forecasting. In *Proceedings of the European Conference on Computer Vision (ECCV)*, 2020. 1, 2, 3, 7

[32] Yicheng Liu, Jinghuai Zhang, Liangji Fang, Qinhong Jiang, and Bolei Zhou. Multimodal motion prediction with stacked transformers. In *Proceedings of the IEEE/CVF Conference on Computer Vision and Pattern Recognition (CVPR)*, 2021. 2, 5, 7

[33] Osama Makansi, Eddy Ilg, Ozgun Cicek, and Thomas Brox. Overcoming limitations of mixture density networks: A sampling and fitting framework for multimodal future prediction. In *Proceedings of the IEEE/CVF Conference on Computer Vision and Pattern Recognition (CVPR)*, 2019. 2

[34] Jean Mercat, Thomas Gilles, Nicole El Zoghby, Guillaume Sandou, Dominique Beauvois, and Guillermo Pita Gil. Multi-head attention for multi-modal joint vehicle motion forecasting. In *Proceedings of the IEEE International Conference on Robotics and Automation (ICRA)*, 2020. 2

[35] Ben Mildenhall, Pratul P Srinivasan, Matthew Tancik, Jonathan T Barron, Ravi Ramamoorthi, and Ren Ng. Nerf: Representing scenes as neural radiance fields for view synthesis. In *Proceedings of the European Conference on Computer Vision (ECCV)*, 2020. 4

[36] Abduallah Mohamed, Kun Qian, Mohamed Elhoseiny, and Christian Claudel. Social-stgcnn: A social spatio-temporal graph convolutional neural network for human trajectory prediction. In *Proceedings of the IEEE/CVF Conference on Computer Vision and Pattern Recognition (CVPR)*, 2020. 2

[37] Nigamaa Nayakanti, Rami Al-Rfou, Aurick Zhou, Kratarth Goel, Khaled S Refaat, and Benjamin Sapp. Wayformer: Motion forecasting via simple & efficient attention networks. *arXiv preprint arXiv:2207.05844*, 2022. 1, 2, 3, 5, 7

[38] Jiquan Ngiam, Benjamin Caine, Vijay Vasudevan, Zhengdong Zhang, Hao-Tien Lewis Chiang, Jeffrey Ling, Rebecca Roelofs, Alex Bewley, Chenxi Liu, Ashish Venugopal, et al. Scene transformer: A unified architecture for predicting multiple agent trajectories. In *Proceedings of the International Conference on Learning Representations (ICLR)*, 2022. 1, 2, 3, 7

[39] Tung Phan-Minh, Elena Corina Grigore, Freddy A Boulton, Oscar Beijbom, and Eric M Wolff. Covernet: Multimodal behavior prediction using trajectory sets. In *Proceedings of the IEEE/CVF Conference on Computer Vision and Pattern Recognition (CVPR)*, 2020. 2, 3

[40] Nicholas Rhinehart, Rowan McAllister, Kris Kitani, and Sergey Levine. Precog: Prediction conditioned on goals in visual multi-agent settings. In *Proceedings of the IEEE/CVF International Conference on Computer Vision (ICCV)*, 2019. 2

[41] Christian Rupprecht, Iro Laina, Robert DiPietro, Maximilian Baust, Federico Tombari, Nassir Navab, and Gregory D Hager. Learning in an uncertain world: Representing ambiguity through multiple hypotheses. In *Proceedings of the IEEE International Conference on Computer Vision (ICCV)*, 2017. 2

[42] Shaoshuai Shi, Li Jiang, Dengxin Dai, and Bernt Schiele. Motion transformer with global intention localization and local movement refinement. In *Advances in Neural Information Processing Systems (NeurIPS)*, 2022. 7

[43] Tong Su, Xishun Wang, and Xiaodong Yang. Qml for argoverse 2 motion forecasting challenge. *arXiv preprint arXiv:2207.06553*, 2022. 7

[44] Matthew Tancik, Pratul Srinivasan, Ben Mildenhall, Sara Fridovich-Keil, Nithin Raghavan, Utkarsh Singhal, Ravi Ramamoorthi, Jonathan Barron, and Ren Ng. Fourier features let networks learn high frequency functions in low dimensional domains. In *Advances in Neural Information Processing Systems (NeurIPS)*, 2020. 4

[45] Yichuan Charlie Tang and Ruslan Salakhutdinov. Multiple futures prediction. In *Advances in Neural Information Processing Systems (NeurIPS)*, 2019. 2

[46] Balakrishnan Varadarajan, Ahmed Hefny, Avikalp Srivastava, Khaled S Refaat, Nigamaa Nayakanti, Andre Cornman, Kan Chen, Bertrand Douillard, Chi Pang Lam, Dragomir Anguelov, et al. Multipath++: Efficient information fusion and trajectory aggregation for behavior prediction. In *Proceedings of the International Conference on Robotics and Automation (ICRA)*, 2022. 1, 2, 3, 5, 7

[47] Ashish Vaswani, Noam Shazeer, Niki Parmar, Jakob Uszkoreit, Llion Jones, Aidan N Gomez, Łukasz Kaiser, and Illia Polosukhin. Attention is all you need. In *Advances in Neural Information Processing Systems (NIPS)*, 2017. 2

[48] Mingkun Wang, Xinge Zhu, Changqian Yu, Wei Li, Yuexin Ma, Ruochun Jin, Xiaoguang Ren, Dongchun Ren, Mingxu Wang, and Wenjing Yang. Ganet: Goal area network for motion forecasting. *arXiv preprint arXiv:2209.09723*, 2022. 7

[49] Benjamin Wilson, William Qi, Tanmay Agarwal, John Lambert, Jagjeet Singh, Siddhesh Khandelwal, Bowen Pan, Ratnesh Kumar, Andrew Hartnett, Jhony Kaesemodel Pontes, Deva Ramanan, Peter Carr, and James Hays. Argoverse 2: Next generation datasets for self-driving perception and forecasting. In *Proceedings of the Neural Information Processing Systems Track on Datasets and Benchmarks (NeurIPS Datasets and Benchmarks)*, 2021. 1, 2, 6

[50] Maosheng Ye, Tongyi Cao, and Qifeng Chen. Tpcn: Temporal point cloud networks for motion forecasting. In *Proceedings of the IEEE/CVF Conference on Computer Vision and Pattern Recognition (CVPR)*, 2021. 1, 2, 7

[51] Maosheng Ye, Jiamiao Xu, Xunnong Xu, Tongyi Cao, and Qifeng Chen. Dcms: Motion forecasting with dual consistency and multi-pseudo-target supervision. *arXiv preprint arXiv:2204.05859*, 2022. 7

[52] Cunjun Yu, Xiao Ma, Jiawei Ren, Haiyu Zhao, and Shuai Yi. Spatio-temporal graph transformer networks for pedestrian trajectory prediction. In *Proceedings of the European Conference on Computer Vision (ECCV)*, 2020. 2

[53] Wenyuan Zeng, Ming Liang, Renjie Liao, and Raquel Urtasun. Lanercnn: Distributed representations for graph-centric motion forecasting. In *Proceedings of the IEEE/RSJ International Conference on Intelligent Robots and Systems (IROS)*, 2021. 2, 3

[54] Chen Zhang, Honglin Sun, Chen Chen, and Yandong Guo. Technical report for argoverse2 challenge 2022–motion forecasting task. *arXiv preprint arXiv:2206.07934*, 2022. 7

[55] Hang Zhao, Jiyang Gao, Tian Lan, Chen Sun, Benjamin Sapp, Balakrishnan Varadarajan, Yue Shen, Yi Shen, Yuning Chai, Cordelia Schmid, et al. Tnt: Target-driven trajectory prediction. In *Proceedings of the Conference on Robot Learning (CoRL)*, 2020. 2, 3

[56] Zikang Zhou, Luyao Ye, Jianping Wang, Kui Wu, and Kejie Lu. Hivt: Hierarchical vector transformer for multi-agent motion prediction. In *Proceedings of the IEEE/CVF Conference on Computer Vision and Pattern Recognition (CVPR)*, 2022. 1, 2, 3, 6, 7